A numerical elastic-thermoviscoplastic model for clay behaviour

David Kurz
KGS Group, 865 Waverley Street, Winnipeg, MB, Canada, R3T 5P4.
Marolo Alfaro, Pooneh Maghoul, Jim Graham
University of Manitoba, Winnipeg, Manitoba, Canada R3T 5V6
Jitendra Sharma
Lassonde School of Engineering, York University,Toronto, Ontario, Canada M3J 1P3

ABSTRACT
Clays exhibit creep in both compression and shear. Viscous behaviour starts immediately after loads are applied and often forms a large component of total deformations. Movements depend on load duration, loading rate, preconsolidation pressure, stress level, the ratio of shear stress to compression stress, strains, strain rate, and temperature. There are also usually small recoverable strains, so the behaviour can be called elastic-thermoviscoplastic (ETVP). The paper outlines a recent ETVP model and describes simulated triaxial test results with different straining rates and temperatures.

RÉSUMÉ
Les argiles présentent un fluage à la fois en compression et en cisaillement. Le comportement visqueux débute immédiatement après l'application des charges et constitue souvent une composante importante des déformations totales. Les mouvements dépendent de la durée de la charge, du taux de chargement, du niveau de contrainte, du rapport de la contrainte de cisaillement à la contrainte de compression, des déformations, de la vitesse de déformation et de la température. Un tel comportement peut aussi être qualifié d'élastique-thermoviscoplastique (ETVP) dès lors que de petites déformations réversibles s'y manifestent. Cet article souligne un modèle récent d'ETVP et décrit les résultats des essais triaxiaux simulés avec des vitesses de déformation ainsi que des températures différentes.

1 INTRODUCTION – VISCOUS BEHAVIOUR

Clays creep: that is, they exhibit viscous behaviour. Creep is seen in long-term settlements of foundations; in settlements and spreading of embankments on soft ground; and in ongoing, often irregular, movements in natural and engineered slopes. It is common in plastic and organic clays (Mitchell and Soga 2005).

Deformations in viscous materials depend on the duration of constant loading, the rate at which loading is applied, the temperature, or some combination of these processes. Creep rates are influenced by stress level, stress rate, strain, strain rate, and temperature. Pre-consolidation pressures, yielding, and undrained shear strengths are all influenced by viscosity (Graham et al. 1983). Viscous behaviour is experienced as non-recoverable straining in compression and shear during both primary consolidation and secondary compression.

Viscous straining involves statistical redistribution of more-stressed and less-stressed inter-particle contacts, and slow movement of 'adsorbed water' close to the surfaces of clay particles (Mitchell and Soga 2005). The combination of load transfer and high viscosity of adsorbed water means that creep movements change with temperature and decay exponentially with time.

2 PARTITIONING OF STRAINS

Creep in clay is commonly thought of as a two-stage process; first, dissipation of excess pore water pressure (primary consolidation), followed by ongoing settlements (secondary compression) (Mesri and Choi 1985).

An alternative approach, which is now favoured, divides settlements into 'instant' and 'delayed' components (Bjerrum 1967). The instant component consists of largely reversible (elastic) deformations of the clay particles. The delayed component is non-recoverable, time-dependent (viscoplastic) reorganization of the inter-particle microstructure. Total strains can then be partitioned into elastic and viscoplastic components. That is, $\{\varepsilon^{total}\} = \{\varepsilon^{elastic}\} + \{\varepsilon^{viscoplastic}\}$ (Yin et al. 2002).

In this second approach, preconsolidation pressures vary with strain rate or with the duration of loading. The slope of Normal Consolidation Lines (NCLs) is constant, but slower loading rates move the lines to lower values of specific volume V (Graham et al. 1983). In the overconsolidated range, unload-reload lines (URLs) and their slopes C_r (or κ) change with strain rate because deformations include both recoverable elastic strains and small viscoplastic non-recoverable strains that vary with the rate and duration of loading (Kelln et al. 2008).

3 EFFECTS OF TEMPERATURE

Effects of changing temperatures must be considered in the design of foundations for furnaces; transmission towers; nuclear waste containment; deep excavations; thermal piles for geothermal energy; and in the effects of climate warming and thawing permafrost under roadways.

In consolidation tests at different temperatures, values of C_r, preconsolidation pressures, and the positions of

NCLs all change with temperature (Campanella and Mitchell 1968, Eriksson 1989).

The effects of viscosity and temperature are similar (Kurz et al. 2016). In particular, values of C_r appear to vary with temperature even if loading rates are constant. This implies that the creep rate coefficient $\psi = dV/d\{ln(t)\}$, changes with temperature. That is $\psi = \psi(T)$, where V is specific volume, t is time, and T is temperature.

Constant-temperature oedometer tests commonly suggest that the coefficient of secondary compression $C_{\alpha e} = dV/d\{log_{10}(t)\}$ varies with over-consolidation ratio (OCR). If viscoplastic straining is due to reorganization of clay particles and adsorbed water, then it should be described by a single parameter ψ that depends on the mineralogy of the clay, the chemistry of the pore fluid, and the temperature. Volume changes can then be described by three material-constant parameters C_r, C_c, and $C_{\alpha e}$ from $\log_{10}$-graphs; or κ, λ, and ψ from ln-graphs. Careful writing of the mathematics of the constitutive model can simulate apparently different values of C_r with changes in stress level, strain rate or temperature.

4 MODELING, TERMINOLOGY AND ASSUMPTIONS

The authors have developed a semi-empirical model that can be calibrated using routine laboratory tests. The model adds viscosity and temperature to Modified Cam Clay (MCC), which is a volumetric-hardening elastic-plastic (EP) model often used in saturated, constant-temperature, constant-chemistry problems where clay can be assumed isotropic and creep movements small.

Effects of temperature have been added to the elastic-viscoplastic (EVP) models described by Yin et al. (2002) and Kelln et al. (2008) that have successfully simulated settlements of large compacted fills. The new model is therefore an elastic-thermoviscoplastic (ETVP) model. Kurz (2014) and Kurz et al. (2016) provide more details.

4.1 Terminology

The terminology is consistent with Wood (1990). This paper deals only with triaxial compression in which $p' = p - u$, where $p = (\sigma_1 + \sigma_2 + \sigma_3)/3$ and σ_1, σ_2, and σ_3 are principal stresses in the axial and radial directions; deviator stress $q = q' = \sigma_1 - \sigma_3$; u is pore water pressure; and V is specific volume.

Subscripts in following sections use i, y, c, cs, m, and x to describe stresses as initial, yield, preconsolidation pressure, critical state, isotropic compression, and current respectively. A point on an NCL is defined by (p'_m, V_m). Superscripts e, p, and vp indicate elastic (recoverable), plastic (non-recoverable), and viscoplastic (time- and temperature-dependent non-recoverable) states.

4.2 Assumptions

The EVP model in Figure 1 assumes that:

1. Elasticity is non-linear and isotropic, with elastic volumetric and shear strains ε_p^e and ε_q^e respectively.
2. Yield envelopes are elliptical and increase with p'_m.
3. The flow rule is 'associated'.
4. A straight hardening law (NCL) has slope λ in V-lnp' - space. Viscosity produces parallel lines with decreasing V as strain rate decreases and temperature increases. These lines are due to additional components of viscoplastic straining.
5. At Critical State, $\partial p'/\partial \varepsilon_q = \partial q/\partial \varepsilon_q = \partial u/\partial \varepsilon_q = \partial V/\partial \varepsilon_q = 0$.
6. Large strain (critical state) failure is defined by the Mohr-Coulomb criterion, where $(\sigma'_1/\sigma'_3)_{max}$ is constant.
7. A single isothermal creep coefficient ψ increases with temperature and denotes rates of viscous compression.

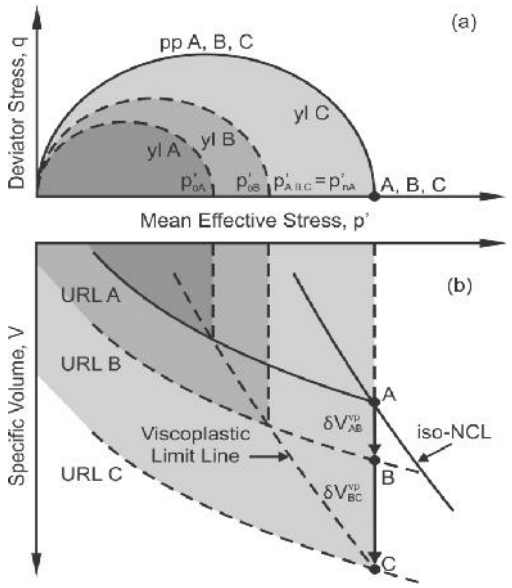

Figure 1. Admissible development of viscoplastic volumetric strains with constant stress for a stress state which resides outside a current yield locus (Kelln 2007).

5 THE EVP FRAMEWORK

Details of the EVP and ETVP model can be found in Kelln et al. (2008), Kurz (2014), and Kurz et al. (2016). Following paragraphs provide a brief overview.

In V,lnp' compression space, the specific volume for a state (p'_m, V_m) at time t can be written:

[1] $$V_m = N - \lambda \ln p'_m - \psi \ln\left(\frac{t_0 + t}{t_0}\right)$$

where N is the intercept of the NCL at a mean stress of p' = 1 kPa, and t is duration of loading. Equation [1] is defined for $t > -t_0$, with $t_0 = 0$ taken at the end of primary consolidation or the commonly used loading interval of 24 hours. Negative values of t allow viscous deformations to be modelled during primary consolidation.

The first two terms in Eqn. [1] calculate V_{ncl} at p'_m. The third calculates viscoplastic compression and is plotted vertically in compression space for a given stress state (p'_m, V_m). An incremental form of Eqn.[1] provides the viscoplastic volumetric strain rate for (p'_m, V_m), (Eqn.[2]):

[2] $$\varepsilon_p^{vp} = \frac{\delta \varepsilon_p^{vp}}{\delta t} = \left(\frac{\psi}{V_m t_0}\right) exp\left(\frac{V_m - N}{-\psi}\right) (p'_m)^{\frac{\lambda}{\psi}}$$

Using an associated flow rule for general (*p',q,V*) states, a scalar multiplier function *S,* and plastic potential *g*, produces an expression for the viscoplastic strain rate:

[3] $\dot{\varepsilon}_{ij}^{vp} = \left(\frac{1}{\nu_m t_0}\right) exp\left(\frac{\nu_m - \Lambda}{\psi}\right) (p'_m)^{\frac{\lambda}{\psi}} \frac{1}{|\partial g/\partial p'|} \left(\frac{\partial g}{\partial \sigma'_{ij}}\right)$

Yin et al. (2002) and Kelln et al. (2008) defined a viscoplastic limit line (vpl) as the boundary in *p'-V* compression space at which viscoplastic straining is first encountered as *p'* increases from low values (Figure 1). To the right of the vpl in the figure, elastic and viscoplastic behaviour are both present. The vpl can be chosen to correspond with anticipated lifetimes of engineering structures. Analyses are not sensitive to this choice.

Relating the vpl to the NCL and a given URL, defines the viscoplastic volumetric strain rate $\dot{\varepsilon}_{ij}^{vp}$ and the scalar function *S* that defines shear strains, Eqns. [4] and [5]:

[4] $\dot{\varepsilon}_{ij}^{vp} = \left(\frac{1}{V_m t_0}\right)\left(\frac{N - \lambda \ln p'_m - V_m}{N - Z}\right)^{\frac{\lambda}{\psi}} exp\left[\frac{N - \lambda \ln p'_m - V_m}{\left(\frac{N - \lambda \ln p'_m - V_m}{N - Z} - 1\right)\psi}\right] \frac{1}{\left|\frac{\partial g}{\partial p'}\right|} \left(\frac{\partial g}{\partial \sigma'_{ij}}\right)$

[5] $S = \left(\frac{1}{V_m t_0}\right)\left(1 - \frac{N - \lambda \ln p'_m - V_m}{N - Z}\right)^{\frac{\lambda}{\psi}} x \; exp\left[\frac{N - \lambda \ln p'_m - V_m}{\left(\frac{N - \lambda \ln p'_m - V_m}{N - Z} - 1\right)\psi}\right] \frac{1}{\left|\frac{\partial g}{\partial p'}\right|}$

Analyses proceed step-wise, so *δq/δp'* can be changed to accommodate transition from consolidation to shear; from drained to undrained shearing; or to user-controlled changes in the effective stress path.

Kelln et al. (2009) used the EVP model in a finite element analysis to simulate deformations under a highway embankment on soft organic clay. Calculated vertical and lateral deformations agreed well with measured values.

In triaxial tests, slower test speeds permit more viscoplastic straining and this produces different stress-strain behaviour. In overconsolidated clay, the elastic-plastic MCC model allows only elastic strains inside the yield locus, whereas EVP and ETVP models include viscoplastic straining. This affects stress-strain behaviour and pore water pressures or volume changes.

6 INCORPORATING TEMPERATURE

Modeling the effects of temperature changes on stress-strain behaviour of clays mostly uses a mechanics-based approach, for example by Laloui and Cekerevac (2008), and Hueckel et al. (2009). The models usually contain large numbers of variables and are difficult to calibrate.

An alternative approach by Graham et al. (2001), defined a semi-empirical development of MCC that associated the effects of heating with the elastic components of MCC and assumed $\kappa = \kappa(T)$. They called it a thermoelastic-plastic (TEP) model. The assumption was incorrect (Crilly 1996). More recently, Kurz (2014) attached the effects of changes in temperature to the viscoplastic component of the strain tensor and not to the elastic component. It is therefore an elastic-thermoviscoplastic (ETVP) model that can simulate non-isothermal behaviour if ψ is varied with temperature. This has not yet been explored in detail.

6.1 Viscosity as a function of temperature

Warmer clay exhibits more creep straining than a cooler clay. Kelln (2007) suggested that the creep rate parameter ψ can be defined as $\psi = \psi(T)$, but did not develop the idea.

Published data for $\psi = \psi(T)$ are limited and in part contradictory (Leroueil and Marques 1996, Burghinoli et al. 2000). This paper uses the exponential relationship proposed by Fox and Edil (1996), with the creep rate coefficient defined by ψ in (Figure 2).

[6] $\psi_2 = \psi_1 exp\{\Omega(T_2 - T_1)\}$

Here, ψ_1 is the creep rate coefficient at temperature T_1, and ψ_2 is the creep rate coefficient at temperature T_2. The material constant Ω is independent of voids ratio, stress level, overconsolidation ratio, and the change in temperature. Different soils have different values of Ω.

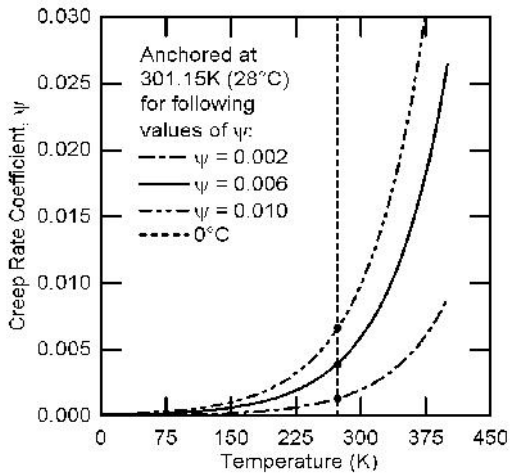

Figure 2. Exponential relationships for the creep rate coefficient ψ versus temperature anchored at a temperature of 28°C, (301.1K) for given values of ψ.

7 IMPLEMENTING $\Psi = \Psi(T)$

Following figures show results from the ETVP model and the $\psi = \psi(T)$ relationship in Figure 2, with conditions in simulations being shown as (ψ,*T)* in the captions. The model simulates drained, undrained, lateral expansion, or user-defined stress paths in triaxial loading. Stresses and strains are calculated in (*q-p'*) space and *V*-ln*(p')* space.

The modeling uses (a) the basic MCC model without temperature or viscous effects ($\psi = 0$); (b) Kelln's (2007) EVP model at (ψ_1, T_1); and (c) the ETVP model at (ψ_2, T_2) as a result of a temperature change $dT = T_2 - T_1$.

7.1 Limitations of the ETVP model

1. The model focuses only on $\psi = \psi(T)$. All other parameters used by Kelln et al. (2008) are unchanged.
2. Thermal expansion and contraction of the soil particles and water is not implemented. Discussions suggest their inclusion in the ETVP model may not be necessary.
3. Phase change is not included.
4. Elastic properties are independent of temperature but change with stress level and specific volume.
5. Parallel 'time lines' and changes in slopes of URLs result from viscoplastic straining relative to a chosen NCL.
6. The material parameter, Ω, is assumed to be Ω = 0.015/°C. Literature related to this value is limited.

7.2 Modeling parameters

Test types and overconsolidation ratios impact soil behaviour considerably. The ETVP model was used in a sensitivity analysis of undrained ($CI\bar{U}$) and drained (CID) triaxial compression tests with three overconsolidation ratios: 1.00 for normally consolidated (NC) clay, 1.67 for lightly overconsolidated (LOC) clay, and 5.00 for heavily overconsolidated (HOC) clay. Modeling used the same material properties as Kelln et al. (2008) (Table 1). This allowed direct comparisons with Kelln's results and also with MCC modeling using $\psi = 0$.

Table 1. Soil parameters used to simulate $CI\bar{U}$ and CID triaxial compression tests.

Soil Parameter	Symbol	Value
Slope of the CSL	M	1.00
Slope of the NCL	λ	0.25
Slope of the URL	κ	0.05
Creep rate coefficient	ψ	0.006
Initial temperature	T_1	28°C
Constant for $\psi = \psi(T)$	Ω	0.015/°C
Origin of the NCL	N	3.00
Origin of the vpl)	Z	1.00
Curve-fitting parameter	t_0	1.00 day
Poisson's ratio	ν'	0.30

Simulations were run with isotropic preconsolidation pressures p'_c of 25.0 kPa and 50.0 kPa; and axial strain rates $d\varepsilon_1/dt$ of 15.0%/day, and 0.15%/day. At the faster rate of 15.0%/day, drainage is not usually complete in drained tests and excess pore water pressures develop. Drained results are only shown for 0.15%/day.

The final variable needed for sensitivity analysis is the creep rate coefficient $\psi = \psi(T)$. Figure 2 needs an 'anchor' value of ψ_1 from a standard creep test at a known laboratory temperature T_1, that is, (ψ_1, T_1). Kurz (2014) used three values of ψ_1 but only results for ψ = 0.006 will be shown. The 'anchor' temperature, T_1 = 28°C allows comparison with TEP results from Graham et al. (2001).

8 REPRESENTATIVE RESULTS

We can show only a small number of graphs of the effects of strain rates and temperature on clay behaviour. More information about clay behaviour associated with the three chosen temperatures and three axial strain rates can be found in Kurz (2014) and Kurz et al. (2016).

Figure 3 shows simulated results from a normally consolidated (NC) specimen sheared with axial strain rate of 15%/day in an undrained ($CI\bar{U}$) triaxial test. Figure 4 is for a heavily overconsolidated (HOC) undrained specimen sheared at 0.15%/day. The figures use the symbol u for *changes* in pore water pressure during shearing. Figure 5 shows results from a simulated drained test on a heavily overconsolidated CID specimen sheared at 0.15%/day.

The graphs show relationships for (a) q vs. p'; (b), V vs. mean effective stresses p' and p'_m; (c) viscoplastic volumetric strain rate $\dot{\varepsilon}_p^{vp}$ vs. p'_m; (d) q vs. ε_q; and (e) u vs. ε_q for the $CI\bar{U}$ tests, and V vs. ε_q for the drained test.

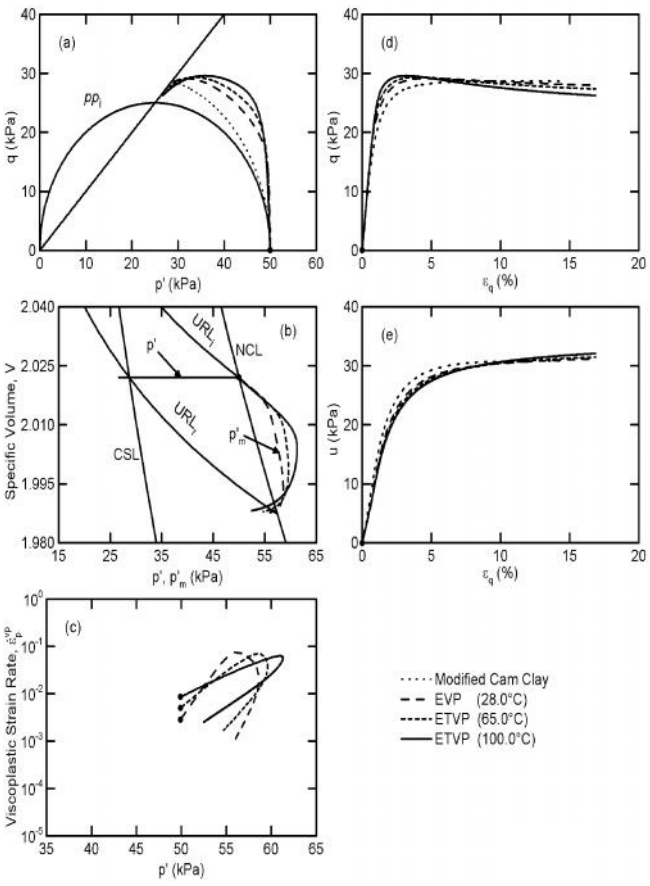

Figure 3. Response of the EVTP model for a $CI\bar{U}$-NC clay at $\dot{\varepsilon}_1$ = 15.0%/day and (ψ_1, T_1) = (0.006,28°).

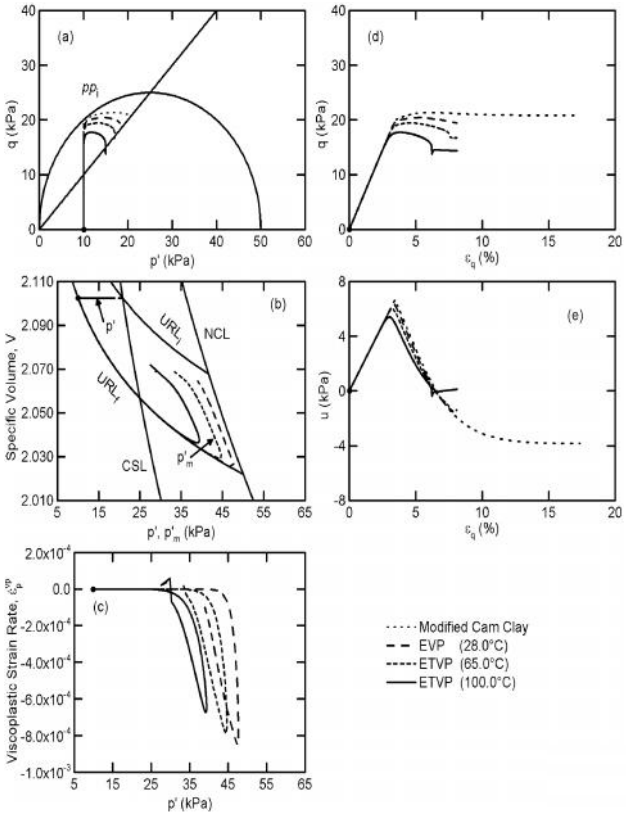

Figure 4. Response of the ETVP model for a CIŪ-HOC clay at $\dot{\varepsilon}_1$ = 0.15%/day and (ψ_1,T_1) = (0.006,28°).

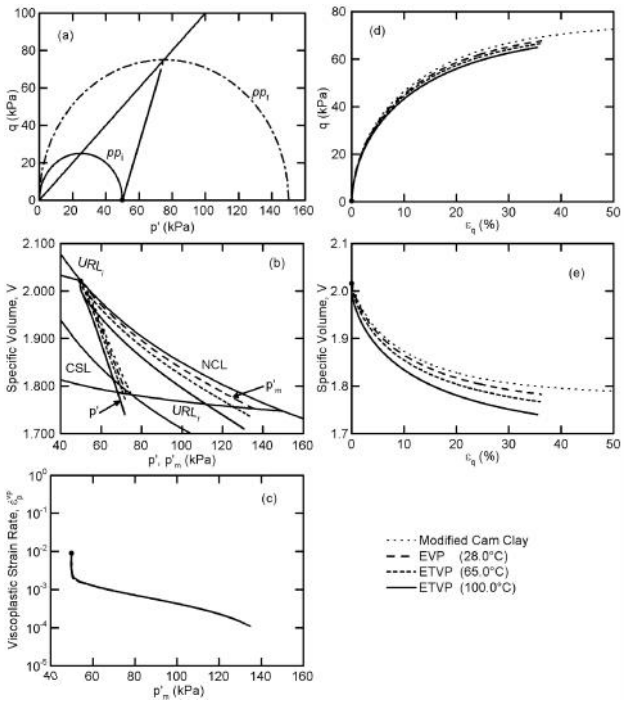

Figure 5. Response of the ETVP model for a CID-NC clay at $\dot{\varepsilon}_1$ = 0.15%/day and (ψ_1,T_1) = (0.006,28°).

Values of p'_m represent viscoplastic hardening and elastic softening. They also show MCC results without viscosity or temperature effects, and ETVP modeling for temperatures of 28°C, 65°C, and 100°C; and ψ_1 = 0.06.

Of particular interest is the strain softening seen in Figures 3 and 4. Deviations from the MCC conditions $\partial p'/\partial \varepsilon_q$, $\partial q/\partial \varepsilon_q$, $\partial u/\partial \varepsilon_q$, and $\partial V/\partial \varepsilon_q = 0$ were larger when the strain rates of the tests were slower and temperatures higher. Longer tests allow the addition of larger thermo-viscoplastic volumetric strains in undrained tests. These must be offset by larger elastic volumetric strains to keep the volume constant. To do this, pore water pressures must increase and p' must decrease. Deviator stresses must therefore decrease if large-strain strengths are to remain on the critical state line CSL. The result is strain softening. Increasing temperatures amplify this effect.

At large axial strains, the measurable variables change slowly and numerical procedures need to divide small values in the equations by other smaller values. As a result, numerical instabilities sometimes developed.

8.1 Modeling Normally Consolidated CIŪ Behaviour

Figure 3 provides insights into ETVP behaviour in undrained tests. In graph (b), the horizontal line that extends leftwards from the isotropic consolidation pressure of 50 kPa on the NCL represents the constant-volume stress path of CIŪ tests. As the simulation proceeds towards peak failure, the volumetric viscoplastic strain rate $\dot{\varepsilon}_p^{vp}$ in (c) increases. So, also, do compensating pore water pressures in (e) and the values of p'_m in (b) that define the size of the plastic potential. After peak shear strength is reached, $\dot{\varepsilon}_p^{vp}$ and p'_m decrease toward end-of-test (large strain) values, and pore water pressures increase. The zero-conditions for Critical States are not reached, but large-strain strengths all lie close to the CSL in (a) with slightly different values of q'_f, p'_f, p'_{mf}, and u_f.

ETVP (and EVP) models generate strain softening due to thermoviscoplastic strains that correspond to changes in the plastic potentials indicated by p'_m in the graphs. Kurz et al. (2016) show that faster straining produces higher peak deviator stresses that increase with temperature. After peak deviator stress, the rate of viscoplastic straining and the plastic potential decrease.

Since volumes are kept constant in CIŪ tests, pore water pressures must increase to offset viscoplastic volumetric compressions.

Due to differences in strain softening related to the changes in p'_m in Figure 3c, higher temperatures produce lower stresses at the End-of-Test (EOT), (Figure 3d). Slower straining produces more visco-plastic behaviour, lower peak deviator stresses, and lower deviator stresses at EOT. Changing strain rates therefore also change effective stress paths and pore water pressures.

8.2 Modeling Overconsolidated CIŪ Behaviour

With some exceptions, simulations of overconsolidated CIŪ tests present broadly similar responses to temperature-dependent viscosity as NC tests. Of course, stress, strain, and pore water pressure relationships depend on over-consolidation ratio (OCR) and details are different. Because strains and their durations are small

before yielding is reached, only small viscoplastic strains occur, although their rate increases as yielding is approached. (Viscoplastic volumetric strain rates are low when overconsolidation ratio OCR is high.) Temperature-dependency is only really apparent after peak strengths have been passed and the differences are small.

The peaks of the pore water pressure graphs do not coincide with the first crossing of the critical state line ($\eta = M$), but instead represent a gradual transition from compressive to expansive behaviour.

Compared with slower strain rates, faster rates produce higher, and increasing, peak deviator stresses as temperatures increase. The differences lie with the responses of the pore water pressures. For incremental stress ratios $\partial q/\partial p'$ below the CSL when $\eta = q/p' < M$, the behaviour is primarily elastic volumetric compression. Pore water pressures therefore increase to keep specific volume constant. Above the CSL line, with $\eta > M$, the behaviour transitions to plastic volumetric expansion, leading eventually to decreasing pore water pressures. This is seen in tests, but is missing in MCC modeling.

8.3 Modeling Drained (CID) Behaviour

Figure 5 shows results for a drained CID-NC test with strain rate 0.15%/day. As with the CIU̅ tests, this slower strain rate allows larger viscoplastic strains to develop than the faster strain rate, which in any case, is unreasonably fast for CID tests. The ETVP model has not yet been coupled with a pore water pressure dissipation model - it simply assumes that tests are run slowly enough that excess pore water pressures do not develop.

As in Eriksson (1989), Figure 5b shows NCLs moving to lower specific volumes at higher temperatures. While the *q-p'* stress path in Figure 5a is the same for all temperatures, both elastic and viscoplastic strains will develop from the start of the test, with consequent changes in p'_m, and temperature-dependent paths in Figures 5b, 5d, and particularly in 5e.

In overconsolidated drained tests, stress paths inside the yield envelope involve both elastic and viscoplastic strains, with corresponding changes in p'_m (Kelln et al. 2008). Subsequently, predominantly plastic responses are related to viscoplastic strain rate and not simply to a sudden transition to a post-yield condition. These features all vary with temperature.

As with CIU̅ simulations, convergence difficulties were seen with the CID-HOC simulations and critical (*p',q,V)* states were usually not achieved. For example, graphs of *q-p'* and *V*-ε_q in figures 5d and 5e continue changing until the simulations were terminated

9 DISCUSSION

It is sometimes thought that the effects of temperature on creep in clay are small. We disagree; although they are commonly smaller than those associated only with creep.

Figure 6 summarizes effects of temperature and strain rate on peak deviator stress q_p and pore water pressure u_p in undrained CIU̅ − HOC simulations. Figure 7 shows related results for CID-HOC simulations. Simulated results for 100°C and 0.15%/d have not been included in Figure 7 due to numerical instabilities in the analyses.

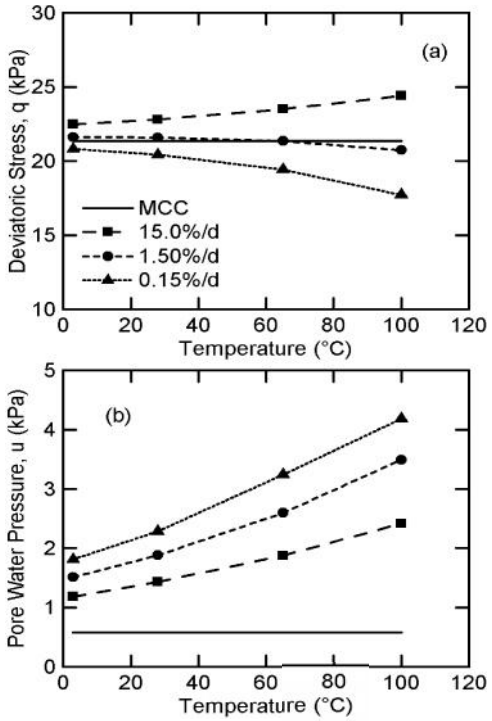

Figure 6. Values of deviator stress q_p and pore water pressure u_p at peak failure for CIU̅ −HOC simulations.

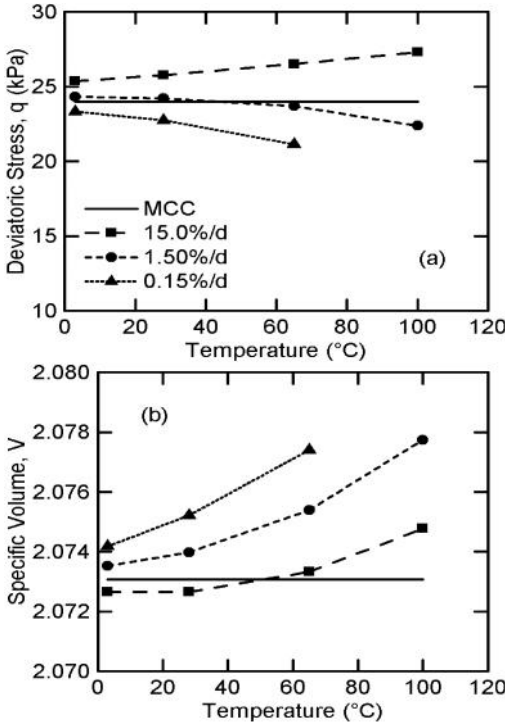

Figure 7. Values of deviator stress *q* and specific volume *V* at peak failure for CID-HOC simulations.

Figure 6 and Figure 7 allow comparison of test results from HOC specimens where viscous effects would be relatively small (T = 28°C, $\dot{\varepsilon}_1$ = 15%/day), and where they would be larger (T = 100°C, $\dot{\varepsilon}_1$ = 0.15%/day). In each case, ψ_1 was 0.006. In $CI\bar{U} - NC$ simulations (not shown), the increased thermoviscoplastic straining produced a decrease of 26.1% in peak deviator stress q_p, and an increase of 51% in $A_p = a_{up}/q_p$. For simulations with overconsolidation ratio 1.67, equivalent differences were 25.9% reduction and 76.3 increase, respectively. The results appear substantial. The figures also show values from MCC that of course do not include the effects of temperature or strain rate.

While this paper has dealt only with single-element, isotropically consolidated triaxial compression tests at various confining pressures, the ETVP model can, in principle, be incorporated into finite element analyses and simulate anisotropic consolidation, step-wise changes in stress path, and the effects of heating or cooling. Further studies are being done and will be reported later.

Earlier discussion showed that apparent changes in slope of unload-reload lines (URLs) with changes in strain rate (Sällfors, G. 1975), and temperature (Eriksson 1989), result from a combination of elastic and viscoplastic straining before yielding is reached. Studies by Graham et al. (2001) produced a thermoelastic-plastic (TEP) model that assumed $\kappa = \kappa(T)$, even though Crilly (1996) showed that κ itself did not vary with temperature. This apparent dependency of κ on temperature combines temperature-independent elasticity and temperature-dependent viscous effects (Kurz 2014). Modeling in this way agrees better with how we currently understand the mechanisms of intra-particle and inter-particle deformations.

Figure 8 shows simulated isotropic consolidation curves at temperatures of 28.0°C and 100.0°C for normally consolidated (NC) specimens and overconsolidated specimens with OCRs of 1.20, 1.67, and 2.00. The creep rate coefficient ψ is again defined by $\psi = \psi(T)$, with $(\psi_1, T_1) = (0.006, 28.0°C)$.

Drawing lines through points of maximum curvature for each OCR for a given temperature suggests that slopes of the initial loading lines, which include thermoviscoplastic behaviour, vary with temperature. The assumption that $\kappa = \kappa(T)$ can therefore be justified in a qualitative, but not physical, sense (Graham et al. 2001).

Figure 8 also shows that the ETVP model simulates preconsolidation pressures that decrease with increasing temperature, and NCLs that move to lower values of specific volume with increasing temperature. This was shown in the laboratory data by Campanella and Mitchell (1968) and Eriksson (1989), among others.

The model can also simulate volume changes in drained tests in which temperatures were increased on specimens having different isotropic consolidation pressures and overconsolidation ratios (OCRs). The TEP and ETVP models produce results that are somewhat different but agree qualitatively with laboratory results from Hueckel and Baldi (1990), (Kurz et al. 2016).

In its current form, the ETVP model has only been validated qualitatively against published data. Quantitative comparisons are not possible, largely because published

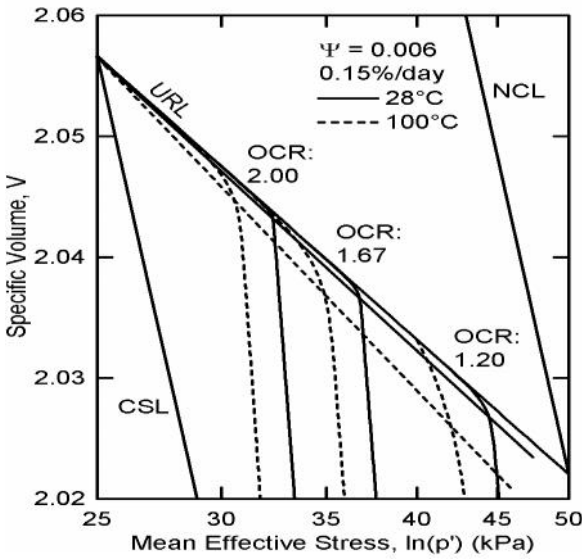

Figure 8. ETVP modeling of compression of overconsolidated specimens with constant κ and temperatures of 28°C and 100°C. The creep rate coefficient ψ is defined by $\psi = \psi(T)$, with $(\psi_1, T_1) = (0.006, 28.0°C)$

data rarely include enough details about specimen preparation and test conditions to all confirmation.

In its present form, the semi-empirical ETVP model can qualitatively simulate laboratory tests with different loading rates and different temperatures. It is now being generalized into a finite element load-deformation model that includes pore water pressure dissipation

10 CONCLUSIONS

The project examined relationships between time, temperature, and load-deformation behaviour in clay. A sensitivity analysis used realistic properties for elastic, normally consolidated, unloading-reloading, creep, yielding, and failure parameters. All the properties can be readily measured in standard laboratory tests.

The research combined thermoplasticity with viscoplasticity into an elastic-thermoviscoplastic (ETVP) model for isotropically consolidated triaxial shear tests. The modeling showed strain softening after peak deviator stress. This is seen in laboratory testing but not in Modified Cam Clay modeling.

The ETVP model is compatible with MCC modeling if ψ is set to zero, and with EVP modeling if the same value of ψ is chosen in both. It can be developed for more general stress states and used in finite element modeling.

ACKNOWLEDGEMENTS

Dr. Curtis Kelln provided helpful advice for developing his EVP model into the ETVP model.

11. REFERENCES

Bjerrum, L. 1967. Engineering geology of Norwegian normally consolidated marine clays as related to settlements of buildings, 7th Rankine Lecture. Géotechnique, **17**(2): 81-118.

Burghinoli, A., Desideri, A., and Miliziano, S. 2000. A laboratory study on the thermomechanical behaviour of clayey soils. Canadian Geotech. J., **37**: 764-780.

Campanella, R.G., and Mitchell, J.K. 1968. Influence of temperature variations on soil behaviour. Journal of the Soil Mechs. and Found. Div. ASCE, **94**: 709-734.

Crilly, T.N. 1996. Unload–reload tests on saturated illite specimens at elevated temperatures. M.Sc. thesis, University of Manitoba, Winnipeg, Man.

Eriksson, L.G. 1989. Temperature effects on consolidation properties of sulphide clays. *In* Proceedings of the 12th Int. Conf. on Soil Mechs. and Found. Eng., Rio de Janeiro, A.A. Balkema, Rotterdam, Netherlands. Vol. 3, pp. 2087-2090.

Fox, P.J. and Edil, T.B. 1996. Effects of stress and temperature on secondary compression of peat. Canadian Geotech. J., **33**: 405-415.

Graham, J., Crooks, J.H.A., and Bell, A.L. 1983. Time effects on the stress-strain behaviour of natural soft clays. Géotechnique, **33**(3): 327-340.

Graham, J., Tanaka, N., Crilly, T. and Alfaro. M. 2001. Modified Cam-Clay modelling of temperature effects in clays. Canadian Geotechnical Journal **38**, 608-621. doi: 10.1139/t00-125.

Hueckel, T., and Baldi, G. 1990. Thermoplasticity of saturated clays: experimental constitutive study. Journal of Geotech. Eng., ASCE, **116**: 1778–1796.

Hueckel, T; Francois, B; Laloui, L. 2009. *Explaining thermal failure in saturated clays,* Géotechnique, **59**: 197-212. doi:10.1680/geot.2009.59.3.197.

Kelln, C.G. 2007. An elastic-viscoplastic constitutive model for soil. Ph.D. thesis. Queen's University Belfast, Belfast, Northern Ireland, UK.

Kelln, C., Sharma, J., Hughes, D, and Graham, J. 2008. An improved elastic-viscoplastic soil model. Canadian Geotech. J., **45**, 1356-1376. doi:10.1139/T08-057.

Kelln, C., Sharma, J., Hughes, D. and Graham, J. 2009. Finite element analysis of an embankment on soft estuarine deposit using an elastic-viscoplastic soil model. Can. Geotech. J. **46**: 357-368.

Kurz, D.R. 2014. Understanding the effects of temperature on the behaviour of clay. PhD thesis, University of Manitoba, Winnipeg, Canada.

Kurz, D., Sharma, J., Alfaro, M., and Graham J. 2016. A semi-empirical elastic-thermoviscoplastic model for clay. Canadian Geotechnical Journal Accepted for publication, May 2016,

Laloui, L., and Cekerevac, C. 2008. Non-isothermal plasticity model for cyclic behaviour of soils. Int. Journal for Numerical and Analytical Methods in Geomechanics **32**: 437-460. doi: 10.1002/nag.629

Leroueil, S. and Marques, M.E.S. 1996. Importance of strain rate and temperature effects in geotechnical engineering, In TC Sheahan, VN Kaliakin (eds.), *Measurement and modeling time dependent soil behaviour, Geotech. Spec. Publ.*, ASCE, Reston, Va.

Mesri, G., and Choi, Y.K. 1985. The uniqueness of end-of-primary (EOP) void ratio effective stress relationship. *In* Proceedings of the 11th International Conference on Soil Mechanics and Foundation Engineering, San Francisco, USA. pp.587-590.

Mitchell, J.K. and Soga, K. 2005. *Fundamentals of Soil Behavior*, 3rd Edition. Wiley and Sons, New York, NY.

Sällfors, G. 1975. Preconsolidation pressure of soft, high-plastic clays. PhD thesis, Chalmers University of Technology, Göteborg, Sweden.

Wood, D.M. 1990. *Soil behaviour and critical state soil mechanics.* Cambridge Univ.Press, Cambridge, UK..

Yin, J.-H., Zhu, J.-G., and Graham, J. 2002. A new elastic viscoplastic model for time-dependent behaviour of normally and overconsolidated clays: theory and verification. Canadian Geotech. J. **39**, 157-173.